JCTC Journal of Chemical Theory and Computation

Article

pubs.acs.org/JCTC

An Extension and Further Validation of an All-Atomistic Force Field for Biological Membranes

Joakim P. M. Jämbeck* and Alexander P. Lyubartsev*

Division of Physical Chemistry, Arrhenius Laboratory, Stockholm University, Stockholm, SE-10691, Sweden

Supporting Information

ABSTRACT: Biological membranes are versatile in composition and host intriguing molecular processes. In order to be able to study these systems, an accurate model Hamiltonian or force field (FF) is a necessity. Here, we report the results of our extension of earlier developed all-atomistic FF parameters for fully saturated phospholipids that complements an earlier parameter set for saturated phosphatidylcholine lipids (*J. Phys. Chem. B*, **2012**, *116*, 3164−3179). The FF, coined Slipids (Stockholm lipids), now also includes parameters for unsaturated phosphatidylcholine and phosphatidylethanolamine lipids, e.g., POPC, DOPC, SOPC, POPE, and DOPE. As the extended set of parameters is derived with the same philosophy as previously applied, the resulting FF has been developed in a fully consistent manner. The capabilities of Slipids are demonstrated by performing long simulations without applying any surface tension and using the correct isothermal−isobaric (*NPT*) ensemble for a range of temperatures and carefully comparing a number of properties with experimental findings. Results show that several structural properties are very well reproduced, such as scattering form factors, NMR order parameters, thicknesses, and area per lipid. Thermal dependencies of different thicknesses and area per lipid are reproduced as well. Lipid diffusion is systematically slightly underestimated, whereas the normalized lipid diffusion follows the experimental trends. This is believed to be due to the lack of collective movement in the relatively small bilayer patches used. Furthermore, the compatibility with amino acid FFs from the AMBER family is tested in explicit transmembrane complexes of the WALP23 peptide with DLPC and DOPC bilayers, and this shows that Slipids can be used to study more complex and biologically relevant systems.

INTRODUCTION

For biological systems, few components are as vital as the cell membrane. The thin double layer keeps the cells intact and controls the transport of matter to and from the cells. The cell membrane is also involved in other important processes such as protein anchoring and cell fusion and division. On a microscopic level, the cell membrane is built up by lipids, sterols, and proteins. Due to the hydrophobic effect, the lipids self-assemble in aqueous solution to form the characteristic double layer structure, where the hydrophilic head groups are in contact with the water and the aliphatic tails are excluded from it. The lipid bilayer furthermore makes up the important matrix in which the proteins reside, and the relationship between these proteins and the surrounding lipids is believed to be of an intimate nature. Cell membranes have very complex compositions, and for mammalian cell membranes, phosphatidylcholines (PC) are most abundant. Other components are phosphatidylethanolamines (PE), sphingomyelins, and cholesterol.[1] The degree of unsaturation of the lipid tails can also differ. For example, 2-oleoyl-1-palmitoyl-*sn*-glycero-3-phosphocholine (POPC) is the most common lipid in animal cells,[2] and lipids having more than one double bond are found in most biological membranes.[3] Model membranes are of interest in experimental studies due to the overwhelming complexity of biological membranes, and the applied techniques are often X-ray and neutron scattering, IR/Raman, and NMR spectroscopy.[4−6]

Computer simulations are ideal for studying the mentioned systems in detail[7,8] due to the difficulties linked to obtaining details of soft matter on an atomistic resolution from experiemental studies.[9] Molecular dynamics (MD) simulations are widely used to study lipid bilayers.[7,10−17] Not only have single component bilayers been simulated but also more complex systems with cholesterol and different lipids[18−22] and membrane-protein complexes.[23−27] A large part of a lot studies is performed on single or double component systems with the aim to fully understand these systems before moving on to more biologically relevant membranes.

In MD simulations, a model Hamiltonian is used, where the potential energy function is usually referred to as a force field (FF). In order to perform simulations that lead to reliable results, the FF must be able to accurately describe all the interactions (inter and intramolecular) in the system. As lipid molecules are of a amphiphilic nature, this has proven to be difficult when studying lipid bilayers in full atomistic detail.[15,28−30] Available FFs that include explicit hydrogens are e.g. CHARMM,[31,32] the general AMBER FF (GAFF),[33] and GLYCAM06.[34] Earlier versions of CHARMM[31] and the current GAFF have had problems describing lipid bilayers in the isothermal−isobaric ensemble (*NPT*),[15,28−30,35,36] which is the correct ensemble in which to perform simulations of lipid bilayers.[11,37,38] If no surface tension was applied or if the area membrane plane was not kept constant, the lipid bilayers often ended up in the gel phase ($L_{\beta'}$ or L_{β}) or the so-called rippled phase (P_{β}), instead of the expected fluid phase (L_{α}). FFs with nonpolar and nonaromatic hydrogens included in their heavier atoms, united atom FFs, have not had these problems.[11,16,39−41]

Received: May 2, 2012
Published: June 26, 2012

We have previously derived an all-atomistic FF that is able to describe fully saturated PC lipids without any of the recently mentioned *ad-hoc* solutions.[42] The properties of fluid lipid bilayers such as area per lipid, bilayer thickness, X-ray and neutron scattering form factors, and NMR deuterium order parameters were reproduced for a range of temperatures when compared to experimental data. As the two former properties are of importance, they do not bear the same significance as the two latter when it comes to verifying the model.[43,44] The importance of form factors and NMR order parameters can be explained by the fact that they are experimental raw data, and no simplifications nor models are needed in their interpretation. The dangers of only relying on, e.g., area per lipid when verifying FFs have been pointed out earlier in the literature.[45,46] In order to address the documented variety in biological membranes,[1] we have now expanded the previous FF to include PC and PE lipids that have one double bond per chain. Studies performed by Martinez-Seara et al.[47] have shown that the position of the double bond is critical for the bilayer structure; however, the parametrization presented here was focused on lipids with the double bond in the 9Z position, which is the most relevant position for biological membranes. By removing two or four hydrogens in the aliphatic tail, the properties of a PC/PE lipid bilayer change drastically: the melting point is lowered,[48,49] the local order changes due to the *cis*-double bonds,[50−53] and the area per lipid is significantly increased.[43,54,55] We follow the same philosophy as in the first iteration of the FF,[42] that is, to keep the empirical inputs to a minimum and to rely as much as possible on high level *ab initio* data. The reader is referred to our previous work[42] for a more in-depth description of our parametrization philosophy. The parameter set presented here together with our previous FF parameters is coined Stockholm lipids (Slipids). A number of properties are compared to experimental data, and the agreement is very good. As a result, the parameters for unsaturated PC and PE lipids are very reliable and are able to describe the correct physical nature of lipid bilayers for a range of temperatures. Due to the problems with GAFF for lipids and the fact that GLYCAM06 overestimates the area per lipid[34] and that the parameters were not extensively tested during the parametrization process, lipid−protein complexes have been difficult to study with the AMBER FFs until now. Cordomí et al.[56] studied the compatibility of the popular Berger lipids with AMBER FFs and concluded that the combination AMBER99SB FF[57] is a reliable combination. However, other studies[58] have shown flaws in the soon 15 year old parameter set proposed by Berger et al. when compared to experiments.[59] Therefore, a more accurate description of the lipids is desirable when studying systems where proteins and lipids are interacting. The parametrization presented here and in our previous work has been performed in a scheme faithful to the one used for the AMBER FFs for biomolecules. The compatibility with three FFs for proteins is investigated here with explicit membrane−protein complex simulations on a microsecond time-scale in order to complement our previous free energy of transfer studies. Results show that Slipids is compatible with these amino acid FFs, and therefore the combinations used presented here are good candidates for simulations of membrane−proteins in the native environment. In the modeling community, these more complex simulations will become more important since the interest in studies is growing.[23,24,60]

METHODS AND MODELS

Parameterization. In accordance with the previously derived FF, we have focused on the hydrophobic tails of the lipids. All parameters describing covalent bonds and angles are taken from the C36 FF[32] as well as torsional and Lennard-Jones parameters for the headgroup and glycerol region. The head group charges for the PC lipids were taken from our previous parametrization of saturated PC lipids. *cis*-5-Decene was chosen as a model compound for the *cis* double bond. The target values for the parametrization were experimental density and heat of vaporization. First, the partial atomic charges for the double bond and its immediate neighbors were computed by averaging the charges from 54 conformations of *cis*-5-decene extracted from a MD simulation in the condensed phase. For the PE headgroup, a similar procedure was applied, and the charges were averaged over 40 conformations taken from a POPE lipid bilayer. The charges for the phosphorus group were constrained to the values obtained previously for the PC headgroup[42] in order to keep the number of parameters to a minimum. The initial MD simulations were performed with parameters from the FF for saturated lipids together with C36 parameters for the double bond and headgroup charges in the case of POPE. New partial atomic charges were computed with DFT using the B3LYP exchange-correlation functional[61−64] together with the cc-pVTZ basis set.[65] The molecules were placed in a polarizable continuum with $\varepsilon = 2.04$ by employing the IEFPCM continuum solvent model.[66,67] Charges were determined by minimizing the difference between the electrostatic potential determined from the wave function and the classical point charges with the restrained electrostatic potential approach (RESP).[68] Once the new partial atomic charges were determined, the values of σ and ε of the Lennard-Jones (LJ) potential were optimized by empirically changing them until the simulations were able to reproduce the experimental target values in a reasonable manner. After partial atomic charges and LJ parameters were altered, the torsional potential had to be refitted as well. Again, *cis*-5-decene was used as a model compound. The CH═CH−CH_2−CH_2 and CH−CH_2−CH_2−CH_2 torsion angles were therefore scanned at a CCSD(T)/cc-pVQZ level of theory, achieved by using the HM-IE extrapolation scheme.[31] All geometries were first optimized using the second-order Møller−Plesset perturbation theory[69] with the cc-pVDZ basis set where the torsion angle of interest was fixed. The fitting procedure can be rationalized as follows: the LJ parameters were adjusted in order to bring the simulations closer to experimental data, and once good agreement was met, the torsional potentials were fitted. To obtain self-consistency, this procedure was repeated for a number of iterations. All quantum mechanical calculations were performed with the Gaussian 09 program suite[70] and the RESP calculations with the Red software.[71]

Simulation Details. A time step of 2 fs was used for all simulations together with the Leap-Frog integrator. The LINCS algorithm[72] was used to constrain all covalent bonds except for the bonds in water where the analytical SETTLE method[73] was applied. As the *NPT* ensemble is recommended for lipid bilayer simulations[11,37,38] this was the ensemble of choice. The pressure was kept constant at one atmosphere by a Parrinello−Rahman barostat[74] with a coupling constant of 10.0 ps and an isothermal compressibility of 4.5×10^{-5} bar^{-1}. The pressure was coupled with a semi-isotropic scheme for the bilayer simulations where the pressure in the *xy* plane (bilayer

plane) is coupled separately from the z direction (bilayer normal). The Nosé−Hoover thermostat[75,76] was used to keep the temperature constant with a coupling constant of 0.5 ps, and the water and membrane were coupled to separate thermostats. Long-range electrostatic interactions were treated by a particle mesh Ewald scheme,[77,78] and the real-space cutoff was 1.4 nm with a Fourier spacing of 0.12 nm and a forth-order interpolation to the Ewald mesh. van der Waals interactions were cut off at 1.5 nm with a switching function from 1.4, and long-range corrections to the pressure and energy were added.

All lipid bilayer simulations were performed with a total number of 128 lipids; 64 in each leaflet and 40 TIP3P water molecules[79] per lipid were used to hydrate the systems. The newly derived parameters were systematically validated in simulations of pure lipid bilayers of DOPC (PC18:1(9Z)/18:1(9Z)), POPC (PC16:0/18:1(9Z)), SOPC (PC18:0/18:1(9Z)), DLPE (PE12:0/12:0), DPPE (PE16:0/16:0), DOPE (PE18(9Z)/18(9Z)), and POPE (PE16:0/18:1(9Z)) at different temperatures. Before production runs, 40 ns long simulations were performed in order to equilibrate the systems. Production runs were 0.5 μs long. In order to test the present FFs' compatibility with the current amino acid FFs, simulations of the WALP23 transmembrane helix were performed with three FFs from the AMBER family: AMBER99SB (ff99SB),[57] AMBER99SB-ILDN (ff99SB-ILDN),[80] and AMBER03 (ff03).[81] All simulations of the transmembrane and lipid complex were performed with 128 lipids and 40 TIP3P water molecules per lipid with the same methodology as described above. The peptide was inserted into lipid bilayers consisting of DLPC and DOPC, resulting in a total of six simulations. The peptide was placed in the membrane manually using VMD[82] followed by 10 000 steps of steepest descent energy minimization where all atoms belonging to the peptide were positionally restrained by a harmonic potential with a force constant of 1000 kJ mol^{-1} nm^{-2}. In a subsequent 5 ns long MD simulation, the lipids were relaxed and the peptide was fully restrained, followed by 2 and 5 ns MD runs with heavy and backbone atoms of the peptide and restrained, respectively. To keep the structure of the transmembrane peptide as intact as possible, a last restrained MD simulation was performed for 5 ns with the C_α-carbons restrained. After the stepwise relaxation of the peptide, a 150 ns long simulation was performed in order to bring the system closer to equilibrium before the production run (which was 1 μs long). The tilt between the helix axis and the membrane normal was computed from the first eigenvector of the C_α-carbons' inertia matrix. A summary of all simulations performed in the present manuscript is presented in Table 1.

All MD simulations were performed with the Gromacs software package[83] (versions 4.5.3 and 4.5.4), and analyses were performed with parts of the MDynaMix software package.[84] Simulation snapshots were rendered with the VMD software package.[82] Neutron scattering factors were computed with the SIMtoEXP software[85] employing the scattering density profile proposed by Kučerka et al.[55]

RESULTS AND DISCUSSION

Derived Force Field Parameters. The results from the Boltzmann averaging of the charges are presented in Figure 1. Our calculations indicate that the electron density around the double bond is higher than in saturated alkanes due to the net charge of −0.09e for the CH group. The net negative charge is then neutralized by the neighboring methylene group. The charges for the PE headgroup are similar to the charges in the C36 FF, but the dipole moment of the headgroup is slightly smaller. A large part of the lipid's constituting atoms bears a charge of zero, which is interesting. As a consequence of this, these interactions sites can be excluded from the construction of neighbor lists and therefore save computational time and decrease the gap in terms of computational cost between AA and UA models of lipids.

Table 1. List of Production Simulations Performed in the Present Study[a]

pure lipid bilayers		
lipid	temperature (K)	time (μs)
DOPC (PC18:1(9Z)/18:1(9Z))	293/303/323/333	0.5
POPC (PC16:0/18:1(9Z))	293/303/323/333	0.5
SOPC (PC18:0/18:1(9Z))	293/303/323/333	0.5
DLPE (PE12:0/12:0)	308	0.5
DPPE (PE16:0/16:0)	343	0.5
DOPE (PE18:1(9Z)/18:1(9Z))	272/298/323	0.5
POPE (PE16:0/18:1(9Z))	303	0.5
transmembrane complexes		
lipid	amino acid force field	time (μs)
DLPC (PC12:0/12:0)	AMBER03	1.0
	AMBER99SB	1.0
	AMBER99SB-ILDN	1.0
DOPC	AMBER03	1.0
	AMBER99SB	1.0
	AMBER99SB-ILDN	1.0

[a]All simulations were performed with 128 lipids and 40 water molecules per lipid if nothing else is stated.

After the parametrization for *cis*-5-decene was finished, the computed density and heat of vaporization (ΔH_{vap}) were calculated, 742.2 ± 0.10 kg m^{-3} and 44.8 ± 0.11 kJ mol^{-1}, respectively. The experimental value[86] for the density is 744.5 kg m^{-3}, which means that the parameters obtained reproduce this property very well. However, for ΔH_{vap} the discrepancy between simulation and experiment is larger, where the experimental value is 42.9 kJ mol^{-1}.[87] It turned out to be very difficult to get ΔH_{vap} closer to the experimental result by varying LJ parameters, because electrostatic interaction from the partial charges around the double bond give a significant contribution to the total interaction energy. Results presented in the following sections show that this does not play a significant role in the lipid bilayer simulations. It is also possible that the rather old value of ΔH_{vap} is underestimated. Chiu et al.[39] also obtained a higher value of ΔH_{vap} in the 43A1-S3 FF, but our value is within better agreement with the experimental data available. Since too strong vdW attractions would affect the lipid bilayer structure and lower the area per lipid,[88] a too attractive LJ potential would have shown this in any subsequent lipid bilayer simulation. In Table 2, it is clear that no area per lipid is underestimated, and therefore we can conclude that it is not very likely that the LJ potential is too attractive (for simulating lipid bilayers). The final LJ, torsional parameters, and torsional profiles are given in Tables S1 and S2 and Figure S4, respectively, in the Supporting Information.

Area and Volume per Lipid and Isothermal Area Compressibility Modulus. In Table 2, the area per lipid (A_L) for the investigated lipids are presented. A_L has been considered to be one of the most fundamental properties for lipid bilayers, and many simulations have aimed at reproducing the area per lipid, although it is known that A_L alone is not sufficient to

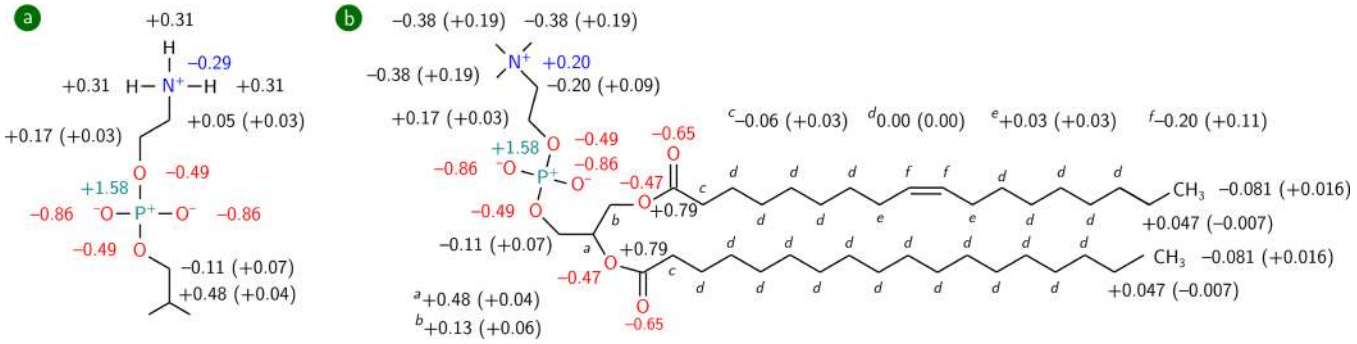

Figure 1. Charges computed for (a) the headgroup of phosphatidylethanolamine lipids and (b) unsaturated phosphatidylcholine lipids. Charges outside the parentheses are on the heavier atoms, and those within denote charges of hydrogens. All charges are given in units of the proton charge.

Table 2. Area per Lipid (A_L), Volume per Lipid (V_L), and Isothermal Area Compressibility Modulus (K_A) from Simulations and Experiments

		A_L nm^2		V_L (nm^3)		K_A (mN m^{-1})	
lipid	temperature (K)	sim.	exptl.	sim.	exptl.	sim.	exptl.
DOPC	293	0.673 ± 0.004	0.691[54a]	1.260	1.288[54a]	282 ± 34	264[54a]
	303	0.680 ± 0.005	0.674[55]	1.262	1.303[54,55]	256 ± 29	184[89]
							254[54]
							265[90]
	323	0.703 ± 0.006	0.755[54b]	1.285	1.318[54b]	246 ± 31	252[54b]
	333	0.714 ± 0.005		1.292		242 ± 36	
POPC	293	0.632 ± 0.005	0.627 ± 0.013[43]	1.200		254 ± 28	
	303	0.646 ± 0.004	0.643 ± 0.013[43]	1.213	1.223[91]	298 ± 30	180−330[92]
					1.256[93]		
	323	0.668 ± 0.006	0.673 ± 0.013[43]	1.235		267 ± 32	
	333	0.682 ± 0.005	0.681 ± 0.014[43]	1.241		272 ± 30	
SOPC	293	0.636 ± 0.004	0.638 ± 0.013[43]	1.268		260 ± 22	290[94a]
	303	0.649 ± 0.005	0.655 ± 0.013[43]	1.270		240 ± 35	200[95]
							290[94d]
	323	0.675 ± 0.006	0.681 ± 0.014[43]	1.294		258 ± 37	
	333	0.687 ± 0.006	0.694 ± 0.014[43]	1.301		244 ± 35	
DLPE	308	0.533 ± 0.003	0.512	0.899	0.942[96]	273 ± 19	
					0.907[4]		
DPPE	342	0.564 ± 0.005	0.605[97]	1.141		271 ± 22	
			0.554[98c]				
DOPE	271	0.572 ± 0.006	0.60[99]	1.157		431 ± 26	
	298	0.604 ± 0.005		1.196		282 ± 23	
POPE	303	0.563 ± 0.004	0.566[95]	1.153		282 ± 29	233[95]

[a]288 K. [b]318 K. [c]Experimental estimate. [d]306 K.

Table 3. Thermal Area Expansivity (α_A^T) and Thermal Contractivity ($\alpha_{D_B}^T$ and $\alpha_{D_C}^T$) from Simulations Compared to Experiments[43] (Reported Values Are Expressed in the Unit K^{-1})

		α_A^T		$\alpha_{D_B}^T$		$\alpha_{D_C}^T$	
lipid	temperature (K)	sim.	exptl.	sim.	exptl.	sim.	exptl.
POPC	293	0.0019	0.0022	0.0012	0.0014	0.0016	0.0011
	303	0.0019	0.0022	0.0012	0.0014	0.0016	0.0011
	323	0.0018	0.0021	0.0013	0.0014	0.0016	0.0011
	333	0.0018	0.0021	0.0013	0.0013	0.0017	0.0011
SOPC	293	0.0020	0.0022	0.0012	0.0014	0.0018	0.0011
	303	0.0020	0.0021	0.0012	0.0014	0.0018	0.0011
	323	0.0019	0.0021	0.0013	0.0014	0.0019	0.0012
	333	0.0019	0.0020	0.0013	0.0015	0.0019	0.0012

judge the quality of a FF.[45,46] Due to the vast number of published experimental values[6] of the areas, which sometimes differ by a few Å^2 for the same lipid under the same conditions, an ensemble of properties from computer simulations should be compared to experimental findings. However, A_L remains an important property to investigate since it gives an indication of

Table 4. Structural Properties of Lipid Bilayers from Simulations and Experiments: Distance between the the Head Groups (D_{HH}), Luzzati Thickness (D_B), and the Hydrophobic Thickness ($2D_C$; All Values Given in nm)

		D_{HH}		D_B		$2D_C$	
lipid	temperature (K)	sim.	exptl.	sim.	exptl.	sim.	exptl.
DOPC	293	3.67	3.76[54a]	3.83		2.96	2.77[54a]
	303	3.66	3.53[89]	3.72	3.59[4]	2.85	2.68[54]
			3.67[55,54]		3.61[89,106]		2.88[55]
			3.69[4]		3.87[55]		
			3.71[106]				
	323	3.55	3.61[54b]	3.66		2.75	2.62[54b]
	333	3.54		3.62		2.75	
POPC	293	3.68		3.89	3.98[43]	2.95	2.92[43]
	303	3.65	3.70[93]	3.85	3.68[93]	2.84	2.88[43]
					3.91[43]		
	323	3.59		3.76	3.79[43]	2.80	2.81[43]
	333	3.54		3.70	3.77[43]	2.74	2.80[43]
SOPC	293	3.82		4.04	4.08[43]	3.01	3.04[43]
	303	3.77	3.92[107]	4.01	4.00[43]	3.06	2.99[43]
	323	3.73		3.93	3.90[43]	2.87	2.93[43]
	333	3.67		3.83	3.85[43]	2.83	2.90[43]
DLPE	308	3.30	3.30[108]	3.39	3.54[96]	2.38	2.58[96]
			3.56[4]				
DPPE	343	4.00		4.04		3.02	3.04[97]
DOPE	272	4.03		4.00		3.39	
	298	3.93		3.82		3.23	
POPE	303	4.11		4.16		3.26	

[a]288 K. [b]318 K.

whether or not the correct phase behavior has been obtained. Further, it is a conceptually convenient property to relate different phenomena to. It is evident that the FF presented here gives values of A_L that are in very good agreement with experiments over a range of temperatures for the PC lipids. For the other headgroup, phosphatidylethanolamine, A_L is within good agreement with the exception of DOPE where A_L is underestimated by roughly 0.03 nm^2. Upon observation, it is clear that the DOPE bilayer does not form a L_β phase although A_L is underestimated. For the rest of the lipids tested here, the agreement with experiments is a very good indication that the lipid bilayers are in the correct phase (L_α). The thermal dependency is also reproduced extremely well. The thermal area expansivity can be calculated from

$$\alpha_A^T = \frac{1}{A_L}\frac{\partial A_L}{\partial T} \quad (1)$$

Results shown in Table 3 are very close to experimental data and show that Slipids can be used at different temperatures. The volume per lipid (V_L) is a less ambiguous property from an experimental point of view, and the values from the simulations in Table 2 compare rather well with the experimental findings. As in the case with saturated lipids, V_L is slightly underestimated with the FF purposed here, which can be attributed to the headgroup parameters.[42]

As simulations proceed, A_L oscillates heavily around the mean value, and from these fluctuations the isothermal area compressibility modulus (K_A) can be computed according to

$$K_A = \frac{2k_B T A_L}{n_L \sigma_A^2} \quad (2)$$

where k_B is the Boltzmann constant, T is the absolute temperature, n_L is the number of lipids, and $\sigma_A{}^2$ is the variance of A_L. In Table 2, values of K_A are presented, and they concord nicely with experimental data. Since fluctuations have to proceed during a relatively long period of time in order to not overestimate K_A,[45] the relatively long sampling time of 0.5 μs was necessary in order to achieve good agreement between simulations and experiments. The size dependency of K_A was not investigated, although there have been suggested methods describing how to deal with these issues.[100] Almost all computed K_A values are within the experimental values when taking the standard deviation into account. As a result of this, we can conclude that mechanical properties are in good agreement with experiments. For DOPE, the isothermal area compressibility modulus decreases significantly when increasing the temperature. As bilayers closer to the gel phase are expected to have higher K_A values, it is likely that the simulation at 271 K was being performed close to a phase transition. This would also explain the slightly too low A_L.

Membrane Thickness. In Table 4, three kinds of membrane thicknesses are presented: the head-to-head distance obtained from electron density profiles (D_{HH}), the Luzzati thickness (D_B), and the hydrophobic thickness ($2D_C$). See the work of Kučerka et al.[101] for definitions of these thicknesses. D_{HH} can be obtained in a rather straightforward manner from X-ray scattering experiments and by inspecting the values obtained from the simulations, it is clear that D_{HH} is reproduced well. Since D_B is defined as the distance between the points along the membrane normal where the water density is half of its bulk value, it can be used as an indicator of the delicate balance between hydrophilic and hydrophobic forces. The fact that the agreement between simulations and experiments for D_B and $2D_C$ is as good as presented in Table 4 shows that these forces are well-balanced. The hydrophobic thickness of a membrane alters the orientation, dynamics, and oligomerization of membrane proteins through so-called

hydrophobic mismatch[102−105] and also affects the passive diffusion of solutes across the membrane. Further on, the ability of the current FF to accommodate a transmembrane helix is investigated. Over a range of temperatures, the thicknesses are reproduced showing that the present FF takes the thermal dependency of the lipid tails and their trans/gauche isomerization into proper account. As the temperature is increased, the disorder of the lipid tails is increased, which leads to an expansion in the membrane plane, and the membrane thickness is decreased. The thermal dependencies of the bilayer thicknesses can be quantified by computing the thermal contractivities $\alpha^T_{D_B}$ and $\alpha^T_{D_C}$ according to

$$\alpha^T_{D_i} = -\frac{1}{D_i}\frac{\partial D_i}{\partial T} \tag{3}$$

Where D_i is D_B or D_C. The data presented in Table 3 show that the simulated bilayers have the correct response to a change in temperature in terms of the Luzzati and hydrophobic thickness.

NMR Order Parameter Profiles and Scattering Form Factors. The local order of a lipid bilayer is described by NMR deuterium order parameters (S_{CD}) according to

$$S_{CD} = \frac{1}{2}\langle 3\cos^2\theta - 1\rangle \tag{4}$$

where θ is the angle between the C−D (actually C−H in the present simulations) vector and membrane normal and the brackets indicate the average during the simulation. The major benefit by studying NMR order parameters for each carbon in the chain of the lipid is that these properties are measured with robust methods, meaning that the results are straightforward to experimentally reproduce. This makes $|S_{CD}|$ a key property in the validation of a FF. In Figure 2, data from simulations of DOPC, POPC, and POPE are compared to experiments.[50−53] It is clear that the three lipid bilayers are in the L_α phase at a temperature of 303 K. In agreement with the findings of Siu et al.,[30] some values of $|S_{CD}|$ for DOPC are slightly overestimated. The significant decrease in chain order for carbons 9 and 10 is due to the position of the *cis* double bond and illustrates the difference between the orientation of the C−H vector of saturated carbons and the C−H vector of unsaturated carbons. The smallest $|S_{CD}|$ values are obtained for the carbons that are located closest to the hydrophobic core of the membrane, which is an important structural property of lipid bilayers, and this has also been seen in previous computer simulations.[30,32,46,109,110] When Siu et al.[30] studied a DOPC bilayer with the popular Berger FF,[11] the *sn*-1 and *sn*-2 tails showed more or less identical $|S_{CD}|$ values, which is in contrast to the findings presented here. For the seven outermost carbons, the order parameters are very similar but around the double bond and at the carbons closest to the glycerol group they differ, which suggests that the two tails are similar but not identical. In the presence of a double bond, the chains orient differently in the lipid bilayer (this is, e.g., illustrated by the differences when comparing $|S_{CD}|$ for the *sn*-1 and *sn*-2 tails for POPC and POPE in Figure 2), and it is clear that the unsaturated *sn*-2 tail is less ordered. The difference in A_L and melting point between saturated and unsaturated lipids can be explained by this, as the latter has a more evident disorder of the lipid tails.

For all lipid types, the splitting of $|S_{CD}|$ for the second carbon of the *sn*-2 tail is present, which is difficult to reproduce with UA FFs.[16,39,40,46] In experiments, it has been observed that the *sn*-1 tail lies in a more perpendicular position relative the bilayer normal than the *sn*-2 tail,[111,112] and as can be seen in Figure 2, this structural feature is also present in the simulations. As a result of this, the *sn*-2 carbonyl dipole interacts with the penetrating water in a more pronounced fashion than the *sn*-1 carbonyl dipole. Observations like these have been made before in both experimental[113,114] and simulation studies.[46]

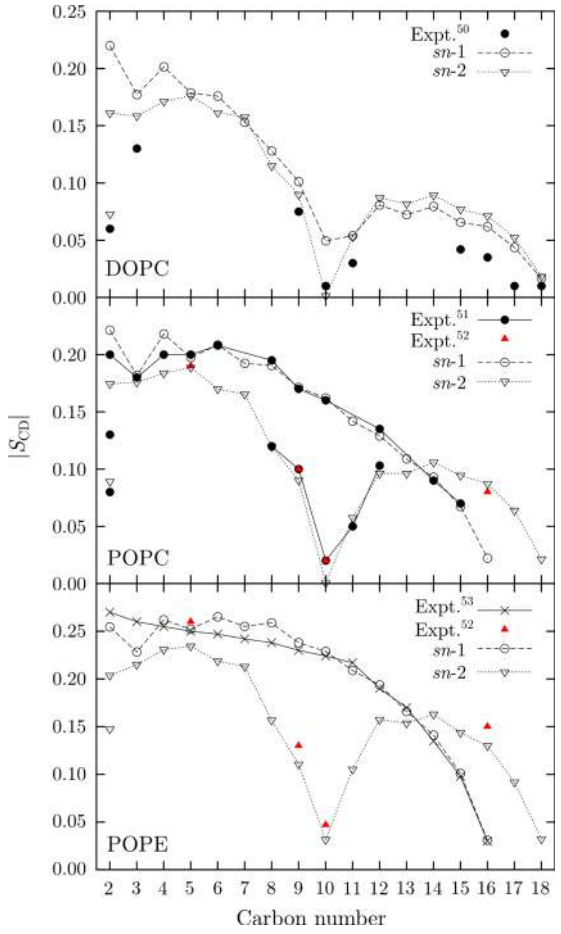

Figure 2. Deuterium order parameter for DOPC, POPC, and POPE lipid bilayers from simulations and experiments.[50−53]

As described above the physical picture of the local orientations of the constituting parts of a lipid can be obtained by computing NMR order parameters. But this structural property does not describe the overall structure of the membrane—in order to do this in a proper manner, one has to investigate scattering form factors, $F(q)$. Since $F(q)$ is obtained directly from experiments, comparisons with simulations serve as an ultimate test of a FF.[43] By computing electron density profiles in the direction of the membrane normal and performing Fourier transformations, $F(q)$ can be obtained from simulations. As can be seen in Figure 3, the computed scattering form factors for DOPC, POPC, and SOPC are in excellent agreement with experimental data.[43,54,55,106,115,116] In Figures S1−S3, the same property is shown for different temperatures, and again the differences between experiments and simulations are negligible. The minima of $F(q)$ are perfectly reproduced in simulations employing the FF presented here and shows that the correct thickness is indeed obtained. The relative lobe heights show that the structure is correct at longer reciprocal distance as well. The agreement with experimental neutron scattering form factors provides further evidence to the present FFs' capabilities

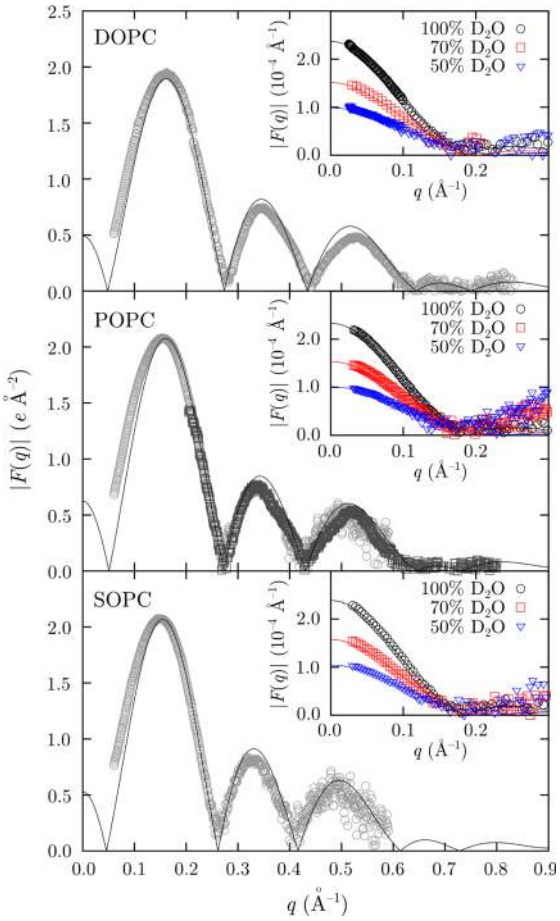

Figure 3. X-ray and neutron (insets) scattering form factors for DOPC, POPC and SOPC from simulations compared to experimental data.[43,54,55,106,115,116] The experimental form factor for DOPC is an averaged data set. Simulation and experimental data are shown as lines and points, respectively.

to describe lipid bilayers. As the scattering form factors are reproduced to such an extent, we can safely assume that all structural data obtained from our simulations are correct.

Lateral Diffusion. The mean-squared displacement (MSD) was used in order to determine the lateral diffusion coefficients D_{lat} according to the Einstein relation

$$D_{lat} = \lim_{t\to\infty} \frac{1}{2n}\frac{d}{dt}\langle|\Delta r_{xy}(t)|^2\rangle = \lim_{t\to\infty} \frac{1}{2n}\frac{d}{dt}\mathrm{MSD}(t) \quad (5)$$

where $n = 2$. The MSD is computed from the center of mass (COM) of the lipids. It has been shown in numerous simulation studies[45,117,118] that the artificial COM of each monolayer results in overestimation of the diffusion, so this contribution was removed before computing D_{lat}. The linear fitting was performed from 0.04 to 0.45 μs of the trajectories. Actual values of D_{lat} are shown in Table S1, and as observed earlier[42] the lateral diffusion is systematically underestimated. The disagreement is largest for the lower temperatures where the diffusion is underestimated roughly by a factor of 2, whereas for the higher temperatures they are underestimated roughly by a factor of 1.5. Despite the disagreement between simulations and experiments, Figure 4 shows that the normalized D_{lat} values are in good agreement, which was also the case for fully saturated lipids.[42] The reason for this could be the lack of collective movements due to thermal density fluctuations in the

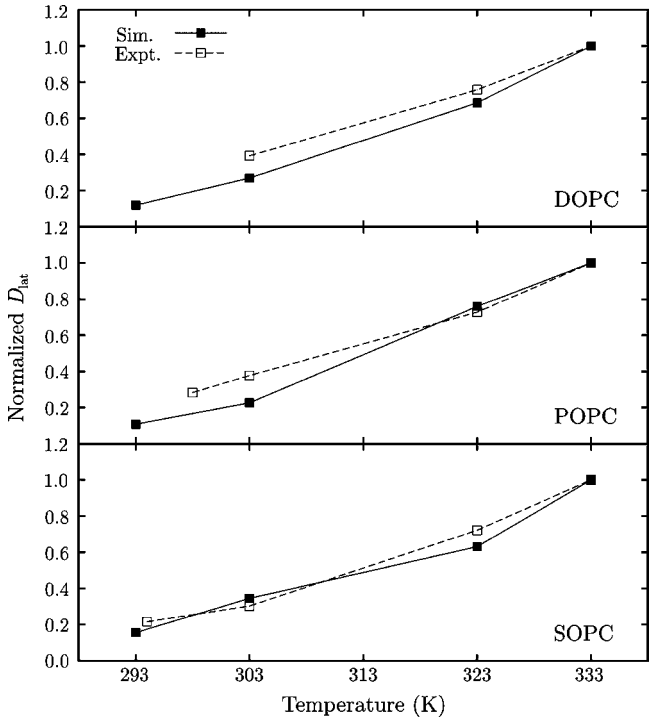

Figure 4. Normalized lateral diffusion coefficients (D_{lat}) from simulations compared to experimental findings.[126,127]

bilayer, which has been observed earlier in simulation[119−121] and experimental studies.[122] This is also similar to the issues highlighted by Yeh and Hummer, who studied the size impact on the diffusion of isotropic liquids.[123] Roark and Feller[120] estimated the correlation length to 2.5 nm, and Falck et al.[119] saw concerted motions on even longer length scales, meaning that larger systems than used in the present investigation (with the typical xy dimensions of 6.4 nm × 6.4 nm) should be used in order to study diffusion. Future work will address the system size dependency of the diffusion coefficients with the focus on short-time local momentum conservation.

The low D_{lat} of DOPE (see Table S3) is related to the fact that the obtained A_L is underestimated. As the area is smaller for the headgroup, it is more difficult for the whole lipid to diffuse since the long time scale diffusion is limited more or less by the headgroup and the avalible 2D-space for it to move within.[124,125]

Transmembrane Helix Tilt. In Table 5, the results of the transmembrane simulations are summarized. Since the helix is of a hydrophobic nature and the lipid bilayers' hydrophobic thicknesses are thinner than the peptide's hydrophobic length, the helix is tilted. When comparing the hydrophobic thicknesses of DLPC and DOPC, 2.06 and 2.96 nm, respectively, it is clear that the helix tilt should be larger in the thinner bilayer in order for the membrane to encapsulate the whole hydrophobic part of the peptide. This has also been verified experimentally[128,129] and in a number of simulation studies.[130−132] With the present FF, it is clear that the helix tilts are close to the experimental values, although the interpretation of these NMR experiments is far from being unambiguous.[128,131,133]

The values reported show that ff99SB performs best together with the lipid parameters; however, it is difficult to rule out the other two amino acid FFs due to the large standard deviations and the relatively short sampling time. Due to the small

Table 5. Average Tilt Angles of WALP23 Described by Three Different Force Fields Embedded in DLPC and DOPC Lipid Bilayers and Areas Per Lipid (A_L)[a]

	peptide tilt (deg)				A_L nm^2	
	DLPC		DOPC		DLPC	DOPC
amino acid force field	sim.	exptl.	sim.	exptl.		
ff99SB	33.2 ± 8.2	35[133]	19.1 ± 7.7	21[133]	0.635 ± 0.006	0.692 ± 0.006
ff99SB-ILDN	40.0 ± 9.1		20.1 ± 7.7		0.637 ± 0.005	0.694 ± 0.005
ff03	39.5 ± 9.4		16.2 ± 7.0		0.637 ± 0.006	0.691 ± 0.006
pure lipid bilayer					0.624 ± 0.004[42]	0.680 ± 0.005

[a]For the lipids, the present force field was used in all cases.

difference between ff99SB and ff99SB-ILDN, it is likely that the (lack of) sampling is the reason for the discrepancy between these FFs. From a qualitative point of view, it is safe to say that all of the AMBER FFs tested here are compatible with our lipid parameters, for both unsaturated and saturated lipids. Values reported by Sapay and Tieleman[134] are close to the values presented here, and Cordomí et al.[56] studied different proteins in lipid bilayers and concluded that ff99SB together with the Berger lipids are a suitable combination. However, the Berger lipids have been found to have a too extended conformation of the headgroup,[58] making this combination less optimal as the headgroup orientation and interactions with the peptide can be very important. The inclusion of a transmembrane helix did not induce any ordering of the lipid bilayers as indicated by the reported A_L in Table 5. This has previously been a problem when mixing lipid and amino acid FFs.[135] A_L is slightly higher than for the pure bilayers, which is to be expected due to the slight expansion of the bilayer in order to facilitate the peptide. The relatively short sampling time (1 μs) can affect the results, which means that the interpretation of the computed values should not be taken too literally. Often simulations on the time scale of ∼5 μs are required to ensure that all thermally relevant points of phase space were visited during the simulations.[131] Further, Neale et al.[136] showed that a single set umbrella sampling simulation lasting for 0.205 μs may not be long enough in order to obtain proper convergence of the standard binding free energy of an amino acid analogue in a DOPC bilayer. We still performed the explicit peptide−membrane simulations in order to obtain a qualitative picture of how the FFs work together.

Another way to determine the compatibility of lipid and amino acid FFs is to compute the free energy of transfer from water to cyclohexane. Cyclohexane is then usually modeled with the Lennard-Jones parameters obtained for the aliphatic lipid tails. However, since it is impossible to capture the collective behavior of the peptide by using merely single amino acid analogues,[137] we only performed simulations of explicit peptides in bilayers.

In Figure 5, the distributions of the peptide tilt angle are shown, and for WALP23 embedded in a DOCP bilayer the distributions for ff99SB and ff99SB-ILDN are slightly wider than for ff03. It is evident that the distributions are not of a Gaussian nature. For the peptide embedded in a thinner DLPC bilayer, the distributions are more of a Gaussian type, although not a strict Gaussian distribution. The nonsymmetric shape obtained with ff03 can probably be attributed to a too short sampling time. The non-Gaussian line shapes obtained for the DOPC bilayers and the Gaussian-like distributions for DLPC have been documented earlier by Monticelli et al.[131] and Wan et al.[132] Since the data presented here do not aim to solve the

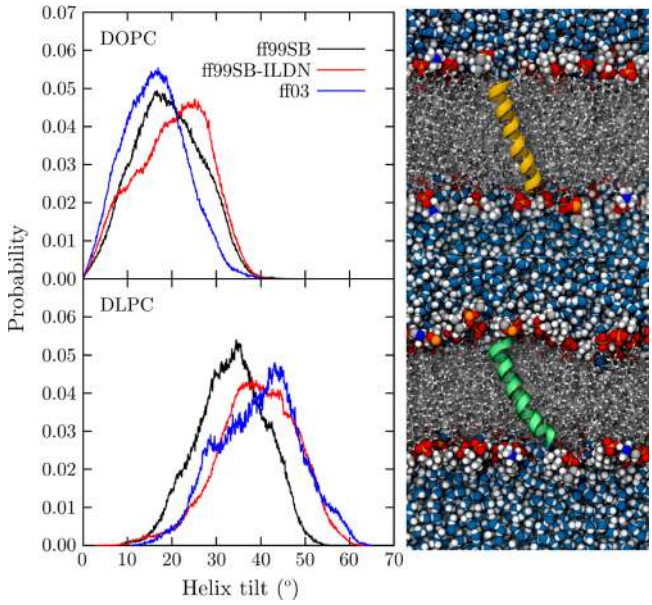

Figure 5. Normalized probability distribution of the peptide tilt angle of a WALP23 peptide embedded in a DOPC (top) and DLPC lipid bilayer (bottom) with the three tested amino acid force fields. To the right, simulation snapshots are shown.

issue of which model should be used when analyzing the motion of peptides in lipid bilayers from experimental data but rather to make qualitative assumptions of the compatibility of the different FFs, we can conclude that all amino acid FFs tested here are compatible with the lipid parameters.

CONCLUSIONS

In order to understand the complex interplay of vital biomolecules, the development of consistent and reliable FFs is necessary. Here, we have taken a second step toward this goal by extending our previous FF for saturated PC lipids[42] by including parameters for unsaturated and PE lipids. As the parameter set is now larger, we referrer to it as Slipids (Stockholm lipids).

The results and discussion presented above show that Slipids is a FF able to describe lipid bilayers accurately under a range of temperatures without an applied surface tension. Analysis of the data presented here shows very good agreement with a number of experimental studies in terms of area per lipid, thickness, and NMR data. Perhaps most important is the scattering form factors,[43] which are perfectly reproduced. Accurate description of structural data is important for future so-called multiscale studies of biological systems,[138] where it is possible to achieve

greater length and time scales in simulations. For these kinds of schemes, a reliable fully atomistic description is a necessity.

We have also presented a broad number of properties that can be and should be used when verifying molecular simulations of lipid bilayers on a atomistic resolution. Similar schemes have been proposed earlier by, e.g., Poger and Mark,[46] but no scattering form factors were discussed there. The inclusion of form factors in the validation goes along with the recommendations of experimental work as well.[43]

The compatibility with popular amino acid FFs makes Slipids an ideal candidate for simulations of more biologically relevant membranes with complex compositions. Current work aims to further extend Slipids to include parameters for cholesterol, anionic lipids, and sphingomyelin in order to make it possible to simulate complex biomolecular systems on a microsecond time scale.

■ ASSOCIATED CONTENT

Supporting Information

Final Lennard-Jones and torsional potential parameters; X-ray scattering form factors for DOPC, POPC, and SOPC at different temperatures; torsional potential profiles; lateral diffusion coefficients; and secondary structure analysis for the WALP23 peptide. A .zip archive includes topologies ready for use with the GROMACS software package as well as force field parameters and coordinates for equilibrated lipid bilayers (also available on http://people.su.se/~jjm).

This material is available free of charge via the Internet at http://pubs.acs.org/.

■ AUTHOR INFORMATION

Corresponding Author

*E-mail: joakim.jambeck@mmk.su.se/jambeck@me.com, alexander.lyubartsev@mmk.su.se. Web site: http://people.su.se/~jjm (J.P.M.J.),http://www.mmk.su.se/~sasha/research.html (A.P.L.).

Notes

The authors declare no competing financial interest.

■ ACKNOWLEDGMENTS

This research has been supported by the Swedish Research Council, grant no. 621-2010-5005. The simulations were performed on resources provided by the Swedish National Infrastructure for Computing (SNIC-003-11-3), at PDC Center for High Performance Computing, High Performance Computing Center North (HPC2N) and National Supercomputer Centre (NSC). We thank A. Rabinovich for fruitful discussions and J. F. Nagle and N. Kučerka for providing experimental data. This work makes use of results produced by the ScalaLife project, a project cofunded by the European Commission (under contract number INFSO-RI-261523). More information on ScalaLife is available at http://www.scalalife.eu.

■ REFERENCES

(1) Wu, N. A. N.; Palczewski, K.; Mu, D. J. *Pharmacol. Rev.* **2008**, *60*, 43−78.
(2) Tattrie, N. H.; Bennet, J. R.; Cyr, R. *Can. J. Biochem.* **1968**, *46*, 819−824.
(3) van der Rest, M. E.; Kamminga, A. H.; Nakano, A.; Anraku, Y.; Poolman, B.; Konings, W. N. *Microbiol. Rev.* **1995**, *59*, 304−322.
(4) Nagle, J. F.; Tristram-Nagle, S. *Biochim. Biophys. Acta* **2000**, *1469*, 159−195.
(5) Vigh, L.; Escribá, P.; Sonnleitner, A.; Sonnleitner, M.; Piotto, S.; Maresca, B.; Horváth, I.; Harwood, J. L. *Prog. Lipid Res.* **2005**, *44*, 303−344.
(6) Nagle, J. F.; Tristam-Nagle, S. *Curr. Opin. Struct. Biol.* **2000**, *10*, 474−480.
(7) Tieleman, D. P.; Berendsen, H. J. C. *J. Chem. Phys.* **1996**, *105*, 4871−4880.
(8) Tieleman, D. P.; Marrink, S. J.; Berendsen, H. J. C. *Biochim. Biophys. Acta* **1997**, *1331*, 235−270.
(9) Kučerka, N.; Liu, Y.; Chu, N.; Petrache, H. I.; Tristram-Nagle, S.; Nagle, J. F. *Biophys. J.* **2005**, *88*, 2626−2637.
(10) Marrink, S. J.; Berendsen, H. J. C. *J. Phys. Chem.* **1994**, *98*, 4155−4168.
(11) Berger, O.; Edholm, O.; Jähnig, F. *Biophys. J.* **1997**, *72*, 2002−2013.
(12) Lindahl, E.; Edholm, O. *Biophys. J.* **2000**, *79*, 426−433.
(13) Falck, E.; Patra, M.; Kartunnen, M.; Hyvönen, M.; Vattulainen, I. *Biophys. J.* **2004**, *87*, 1076−1091.
(14) de Vries, A. H.; Chandrasekhar, I.; van Gunsteren, W. F.; Hünenberger, P. H. *J. Phys. Chem. B* **2005**, *109*, 11643−11652.
(15) Högberg, C.-J.; Nikitiin, A. M.; Lyubartsev, A. P. *J. Comput. Chem.* **2008**, *29*, 2359−2369.
(16) Ulmschneider, J. P.; Ulmschneider, M. B. *J. Chem. Theory Comput.* **2009**, *5*, 1803−1813.
(17) Lyubartsev, A. P.; Rabinovich, A. L. *Soft Matter* **2011**, *7*, 25−39.
(18) Niemelä, P. S.; Hyvönen, M. T.; Kartunnen, M.; Vattulainen, I. *PLoS ONE* **2007**, *3*, e34.
(19) Berkowitz, M. L. *Biochim. Biophys. Acta* **2009**, *1788*, 86−96.
(20) Hall, A.; Róg, T.; Kartunnen, M.; Vattulainen, I. *J. Phys. Chem. B* **2010**, *114*, 7797−7807.
(21) de Joannis, J.; Coppock, P. S.; Yin, F.; Mori, M.; Zamorano, A.; Kindt, J. T. *J. Am. Chem. Soc.* **2011**, *133*, 3625−3634.
(22) Perlmutter, J. D.; Sachs, J. N. *J. Am. Chem. Soc.* **2011**, *133*, 6563−6577.
(23) Gumbart, J.; Wang, Y.; Aksimebtiev, A.; Tajkhorshid, E.; Schulten, K. *Curr. Opin. Struct. Biol.* **2005**, *15*, 423−431.
(24) Lindahl, E.; Sansom, M. S. P. *Curr. Opin. Struct. Biol.* **2008**, *18*, 425−431.
(25) Bjelkmar, P.; Niemelä, P. S.; Vattulainen, I.; Lindahl, E. *PLoS ONE* **2009**, *5*, e1000289.
(26) Ulmschneider, J. P.; Smith, J. C.; White, S. H.; Ulmschneider, M. B. *J. Am. Chem. Soc.* **2011**, *133*, 15487−15495.
(27) Gumbart, J.; Roux, B. *Biophys. J.* **2012**, *102*, 795−801.
(28) Hyvönen, M. T.; Kovanen, P. T. *Eur. Biophys. J.* **2005**, *34*, 294−305.
(29) Sonne, J.; Jensen, M. O.; Hansen, F. Y.; Hemmingsen, L.; Peters, G. *Biophys. J.* **2007**, *92*, 4157−4167.
(30) Siu, S. W. I.; Vácha, R.; Jungwirth, P.; Böckmann, R. A. *J. Chem. Phys.* **2008**, *128*, 125103.
(31) Klauda, J. B.; Brooks, B. R.; MacKerell, J. A. D.; Venable, R. M.; Pastor, R. W. *J. Phys. Chem. B* **2005**, *109*, 5300−5311.
(32) Klauda, J. B.; Venable, R. M.; Freites, J. A.; O'Connor, J. W. O.; Tobias, D. J.; Mondragon-Ramirez, C.; Vorobyov, I.; MacKerell, A. D., Jr.; Pastor, R. W. *J. Phys. Chem. B* **2010**, *114*, 7830−7843.
(33) Wang, J.; Wolf, R. M.; Caldwell, J. W.; Kollman, P. A.; Case, D. A. *J. Comput. Chem.* **2004**, *25*, 1157−1174.
(34) Tessier, M. B.; DeMarco, M. L.; Yongye, A. B.; Woods, R. J. *Mol. Simul.* **2008**, *34*, 349−363.
(35) Jójart, B.; Martinek, T. A. *J. Comput. Chem.* **2007**, *28*, 2051−2058.
(36) Rosso, L.; Gould, I. R. *J. Comput. Chem.* **2008**, *29*, 24−37.
(37) Jähnig, F. *Biophys. J.* **1996**, *71*, 1348−1349.
(38) Marrink, S. J.; Mark, A. E. *J. Phys. Chem. B* **2001**, *105*, 6122−6172.
(39) Chiu, S.-W.; Pandit, S. A.; Scott, H. L.; Jakobsson, E. *J. Phys. Chem. B.* **2009**, *113*, 2748−2763.
(40) Kukol, A. *J. Chem. Theory Comput.* **2009**, *5*, 615−626.
(41) Poger, W. F.; van Gunsteren, D.; Mark, A. E. *J. Comput. Chem.* **2010**, *31*, 1117−1125.

(42) Jämbeck, J. P. M.; Lyubartsev, A. P. *J. Phys. Chem. B* **2012**, *116*, 3164−3179.
(43) Kučerka, N.; Nieh, M.-P.; Katsaras, J. *Biochim. Biophys. Acta* **2011**, *1808*, 2761−2771.
(44) Vermeer, L. S.; de Groot, B. L.; Reat, V.; Milon, A.; Czaplicki, J. *Eur. Biophys. J.* **2007**, *36*, 919−931.
(45) Anézo, C.; de Vries, A. H.; Höltje, H. D.; Tieleman, D. P.; Marrink, S. J. *J. Phys. Chem. B* **2003**, *107*, 9424−9433.
(46) Poger, D.; Mark, A. E. *J. Chem. Theory Comput.* **2010**, *6*, 325−336.
(47) Martinez-Seara, H.; Róg, T.; Pasenkiewicz-Gierula, M.; Vattulainen, I.; Karttunen, M.; Reigada, R. *J. Chem. Phys. B* **2007**, *111*, 11162−11168.
(48) Lewis, R. N. A.; Sykes, B. D.; McElhaney, R. N. *Biochemistry* **1988**, *27*, 880−887.
(49) Huang, C. H.; Lapides, J. R.; Levin, I. W. *J. Am. Chem. Soc.* **1982**, *104*, 5926−5930.
(50) Warschawski, D. E.; Devaux, P. F. *Eur. Biophys. J.* **2005**, *34*, 987−996.
(51) Seelig, J.; Waespe-Sarcevic, N. *Biochemistry* **1978**, *17*, 3310−3315.
(52) Perly, B.; Smith, I. C. P.; Jarrell, H. C. *Biochemistry* **1985**, *24*, 1055−1063.
(53) Raza Shaikh, S.; Brzustowicz, M. R.; Gustafson, N.; Stillwell, W.; Wassall, S. R. *Biochemistry* **2002**, *41*, 10593−10602.
(54) Pan, J.; Tristam-Nagle, S.; Kučerka, N.; Nagle, J. F. *Biophys. J.* **2008**, *94*, 117−124.
(55) Kučerka, N.; Nagle, J. F.; Sachs, J. N.; Feller, S. E.; Pencer, J.; Jackson, A.; Katsaras, J. *Biophys. J.* **2008**, *95*, 2356−2367.
(56) Cordomí, A.; Caltabiano, G.; Pardo, L. *J. Chem. Theory Comput.* **2012**, *8*, 948−958.
(57) Hornak, V.; Abel, R.; Okur, A.; Strockbine, B.; Roitberg, A.; Simmerling, C. *Proteins* **2006**, *65*, 712−725.
(58) Prakash, P.; Sankararamakrishnan, R. *J. Comput. Chem.* **2010**, *31*, 266−277.
(59) Akutsu, H.; Nagamori, T. *Biochemistry* **1991**, *30*, 4510−4516.
(60) Ash, W. L.; Zlomislic, M. R.; Oloo, E. O.; Tieleman, D. P. *Biochim. Biophys. Acta* **2004**, *1666*, 158−189.
(61) Becke, A. D. *J. Chem. Phys.* **1993**, *98*, 5648−5652.
(62) Lee, C.; Wang, W.; Parr, R. G. *Phys. Rev. B* **1988**, *37*, 785−789.
(63) Vosko, S. H.; Wilk, L.; Nusair, M. *Can. J. Phys.* **1980**, *58*, 1200−1211.
(64) Stephens, P. J.; Devlin, F. J.; Chabalowski, C. F.; Frisch, M. J. *J. Phys. Chem.* **1994**, *98*, 11623−11627.
(65) Kendall, R. A.; Dunning, T. H.; Harrison, R. J. *J. Chem. Phys.* **1992**, *96*, 6796−6806.
(66) Tomasi, J.; Mennucci, B.; Cancés. *THEOCHEM* **1999**, *464*, 211−226.
(67) Pomelli, C. S.; Tomasi, J.; Barone, V. *Theor. Chem. Acc.* **2001**, *105*, 446−451.
(68) Bayly, C. I.; Cieplak, P.; Cornell, W.; Kollman, P. A. *J. Phys. Chem.* **1993**, *97*, 10269−10280.
(69) M, C.; Plesset, M. S. *Phys. Rev.* **1934**, *46*, 0618−0622.
(70) Frisch, M. J. et al. *Gaussian 09*, Revision A.02; Gaussian Inc.: Wallingford, CT, 2009.
(71) Dupradeau, F. Y.; Pigache, A.; Zaffran, T.; Savineau, C.; Lelong, R.; Grivel, N.; Lelong, D.; Rosanski, W.; Cieplak, P. *Phys. Chem. Chem. Phys.* **2010**, *12*, 7821−7839.
(72) Hess, H.; Bekker, B.; Berendsen, H. J. C.; Fraaije, J. G. E. M. *J. Comput. Chem.* **1997**, *18*, 1463−1472.
(73) Miyamoto, S.; Kollman, P. A. *J. Comput. Chem.* **1992**, *13*, 952−962.
(74) Parrinello, M.; Rahman, A. *J. Appl. Phys.* **1981**, *52*, 7182−7190.
(75) Nosé, S. *J. Chem. Phys.* **1984**, *81*, 511−519.
(76) Hoover, W. G. *Phys. Rev. A* **1985**, *31*, 1695−1697.
(77) Darden, T.; York, D.; Pedersen, L. *J. Chem. Phys.* **1993**, *98*, 10089−10092.
(78) Essmann, U.; Perera, L.; Berkowitz, T.; Pedersen, L. G. *J. Chem. Phys.* **1995**, *103*, 8577−8593.
(79) Jorgensen, W. L.; Chandrasekhar, J.; Madura, J. D.; Impey, R. W.; Klein, M. L. *J. Chem. Phys.* **1983**, *79*, 926−935.
(80) Lindorff-Larsen, K.; Piana, S.; Palmo, K.; Maragakis, P.; Klepis, J. L.; Dror, R. O.; Shaw, D. E. *Proteins* **2010**, *78*, 1950−1958.
(81) Duan, Y.; Wu, C.; Chowdhury, S.; Lee, M. C.; Xiong, G.; Zhang, W.; Yang, R.; Cieplak, P.; Luo, R.; Lee, T.; Caldwell, J.; Wang, J.; Kollman, P. *J. Comput. Chem.* **2003**, *24*, 1999−2012.
(82) Humphrey, W.; Dalke, A.; Schulten, K. *J. Mol. Graphics* **1996**, *14*, 33−38.
(83) Hess, B.; Kutzner, C.; van der Spool, D.; Lindahl, E. *J. Chem. Theory Comput.* **2008**, *4*, 435−447.
(84) Lyubartsev, A. P.; Laaksonen, A. *Comput. Phys. Commun.* **2000**, 565−589.
(85) Kučerka, N.; Katsaras, J.; Nagle, J. F. *J. Membr. Biol.* **2010**, *235*, 43−50.
(86) Lide, D. R. *CRC Handbook of Chemistry and Physics*, 90th ed.; CRC Press: Boca Raton, FL, 2010; Chapter 3, p 136.
(87) Chickos, J. S.; Acree, W. E., Jr. *J. Phys. Chem. Ref. Data* **2003**, *32*, 1880−2002.
(88) Wohlert, J.; Edholm, O. *Biophys. J.* **2004**, *87*, 2433−2445.
(89) Tristam-Nagle, S.; Petrache, H. I.; Nagle, J. F. *Biophys. J.* **1998**, *75*, 917−925.
(90) Rawicz, W.; Olbrich, K. C.; McIntosh, T.; Needham, D.; Evans, E. *Biophys. J.* **2000**, *79*, 328−339.
(91) Pabst, G.; Rappolt, M.; Amenitsch, H.; Laggner, P. *Phys. Rev. E* **2000**, *62*, 4000−4009.
(92) Binder, H.; Gawrisch, K. *J. Phys. Chem. B* **2001**, *105*, 12378−12390.
(93) Kučerka, N.; Tristam-Nagle, S.; Nagle, J. F. *J. Membr. Biol.* **2005**, *208*, 193−202.
(94) Rawicz, W.; Smith, B. A.; McIntosh, T. J.; Simon, S. A.; Evans, E. *Biophys. J.* **2008**, *94*, 4725−4736.
(95) Rand, R. P.; Parsegian, V. A. *Biochim. Biophys. Acta* **1989**, *988*, 351−376.
(96) Nagle, J. F.; Wiener, M. C. *Biochim. Biophys. Acta* **1988**, *942*, 1−10.
(97) Petrache, H. I.; Dodd, S. W.; Brown, M. F. *Biophys. J.* **2000**, *79*, 3172−3192.
(98) Thurmond, R. L.; Dodd, S. W.; Brown, M. F. *Biophys. J.* **1991**, *59*, 108−113.
(99) Gawrisch, K.; Parsegian, V. A.; Hajduk, D. A.; Tate, M. W.; Gruner, S. M.; Fuller, N. L.; Rand, R. P. *Biochemistry* **1992**, *31*, 2856−2864.
(100) Waheed, Q.; Edholm, O. *Biophys. J.* **2009**, *97*, 2754−2760.
(101) Kučerka, N.; Gallová, J.; Uhríková, D.; Balgavý, P.; Baluca, M.; Marrink, S. J.; Katsaras, J. *Biophys. J.* **2009**, *97*, 1926−1932.
(102) Harroun, T. A.; Heller, W. T.; Wiess, T. M.; Yang, I.; Huang, H. W. *Biophys. J.* **1999**, *76*, 937−945.
(103) Killian, J. A. *Biochim. Biophys. Acta* **1998**, *1376*, 401−415.
(104) Mouritsen, O. G.; Bloom, M. *Biophys. J.* **1984**, *46*, 141−153.
(105) Dumas, F.; Lebrun, M. C.; Tocanne, J. F. *FEBS Lett.* **2010**, *99*, 271−277.
(106) Liu, Y.; Nagle, J. F. *Phys. Rev. E* **2004**, *69*, 040901.
(107) Pan, J.; Tristam-Nagle, S.; Nagle, J. F. *Phys. Rev. E* **2008**, *80*, 021931.
(108) McIntosh, T. J.; Simon, S. A. *Biochemistry* **1986**, *25*, 4948−4952.
(109) Taylor, J.; Whiteford, N. E.; Bradley, G.; Watson, G. W. *Biochim. Biophys. Acta* **2009**, *1788*, 638−649.
(110) Hénin, J.; Shinoda, W.; Klein, M. L. *J. Phys. Chem. B* **2008**, *112*, 7008−7015.
(111) Hitchcook, P. B.; Mason, R.; Thomas, K. M.; Shipley, G. G. *Proc. Natl. Acad. Sci. U.S.A.* **1974**, *71*, 3036−3040.
(112) Seelig, A.; Seelig, J. *Biochim. Biophys. Acta* **1975**, *406*, 1−5.
(113) Wong, P. T. T.; Mantsch, H. H. *Chem. Phys. Lipids* **1988**, *46*, 213−224.
(114) Hübner, W.; Blume, A. *Chem. Phys. Lipids* **1998**, *123*, 99−123.
(115) Kučerka, N.; Tristam-Nagle, S.; Nagle, J. F. *J. Membr. Biol.* **2006**, *208*, 193−202.

(116) Pan, J.; Mills, T. T.; Tristam-Nagle, S.; Nagle, J. F. *Phys. Rev. Lett.* **2008**, *100*, 198103.
(117) Lindahl, E.; Edholm, O. *J. Chem. Phys.* **2001**, *115*, 4938−4950.
(118) Högberg, C. J.; Lyubartsev, A. P. *J. Phys. Chem. B* **2006**, *110*, 14326−14336.
(119) Falck, E.; Róg, T.; Karttunen, M.; Vattulainen, I. *J. Am. Chem. Soc.* **2008**, *130*, 44−45.
(120) Roark, M.; Feller, S. E. *J. Phys. Chem. B* **2009**, *113*, 13229−13234.
(121) Apajalahti, T.; Niemelä, P.; Nedumpully Govindan, P.; Miettinen, M. S.; Salonen, E.; Marrink, S. J.; Vattulainen, I. *Faraday Discuss.* **2010**, *144*, 411−430.
(122) Busch, S.; Smuda, C.; Pardo, L. C.; Unruh, T. *J. Am. Chem. Soc.* **2010**, *132*, 3232−3233.
(123) Yeh, I. C.; Hummer, G. *J. Phys. Chem. B* **2004**, *108*, 15873−15879.
(124) Wohlert, J.; Edholm, O. *J. Chem. Phys.* **2006**, *125*, 204703.
(125) Flenner, E.; Das, J.; Rheinstädter; Koztin, I. *Phys. Rev. E* **2009**, *79*, 011907.
(126) Filippov, A.; Öradd, G.; Lindblom, G. *Langmuir* **2003**, *19*, 6397−6400.
(127) Filippov, A.; Öradd, G.; Lindblom, G. *Biophys. J.* **2007**, *93*, 3182−3190.
(128) Strandberg, E.; Esteban-Martn, S.; Salgado, S.; Ulrich, A. S. *Biophys. J.* **2009**, *96*, 3223−3232.
(129) Esteban-Martn, S.; Giménez, D.; Fuertes, G.; Salgado, J. *Biochemistry* **2009**, *48*, 11441−11448.
(130) Kim, T.; Im, W. *Biophys. J.* **2010**, *99*, 175−183.
(131) Monticelli, L.; Tieleman, D. P.; Fuchs, P. F. J. *Biophys. J.* **2010**, *99*, 1455−1464.
(132) Wan, C. K.; Han, W.; Wu, Y. D. *J. Chem. Theory Comput.* **2012**, *8*, 300−313.
(133) Strandberg, E.; Esteban-Martn, S.; Ulrich, A. S.; Salgado, J. *Biochim. Biophys. Acta* **2012**, *1818*, 1242−1249.
(134) Sapay, N.; Tieleman, D. P. *J. Comput. Chem.* **2011**, *32*, 1400−1410.
(135) Tieleman, D. P.; MacCallum, J. L.; Ash, W. L.; Kandt, C.; Xu, Z.; Monticelli, L. *J. Phys.: Condens. Matter* **2006**, *18*, S1221−S1234.
(136) Neale, C.; Bennett, W. F. D.; Tieleman, D. P.; Pomès, R. *J. Chem. Theory Comput.* **2011**, *7*, 4175−4188.
(137) König, G.; Boresch, S. *J. Phys. Chem. B.* **2009**, *113*, 8967−8974.
(138) Lyubartsev, A. L. *Eur. Biophys. J.* **2005**, *35*, 53−61.